Combustion Properties of MgO for UVA Emission

by

Jia Yu Lin, B.S.

A Thesis

In

Mechanical Engineering

Submitted to the Graduate Faculty
of Texas Tech University in
Partial Fulfillment of
the Requirements for
the Degree of

MASTER OF SCIENCE

Approved

Dr. Michelle Pantoya
Chair of Committee

Dr. Stephen Ekwaro-Osire

Mark Sheridan
Dean of the Graduate School

August, 2017

ACKNOWLEDGMENTS

I sincerely appreciate my research advisor, Dr. Michelle Pantoya, for her encouragement, guidance, and efforts to promote my success, providing me such tremendous help and giving me this opportunity to learn and grow here at Texas Tech University. I would also like to thank Dr. Stephen Ekwaro-Osire for being one of my committee members. Finally, I would like to thank Richa Padhye, Jena McCollum, and Billy Clark for their assistance with my research.

TABLE OF CONTENTS

ABSTRACT

The goal of this study is to formulate a pyrotechnic mixture that emits strongly in the ultraviolet (specifically, UVA) spectrum (i.e., 315-400 nm). This goal was accomplished by testing several formulations using a UV-VIS spectrometer to examine emission spectra upon combustion. The candidate formulations used either aluminum or magnesium powders as the fuel material and were combined with several different solid oxidizers to synthesize a total of 17 candidate formulations. Results showed that the high temperature emission of magnesium oxide was the key ingredient for enhancing UVA emission. Thermal equilibrium chemical modeling using REAL code software shows that the flame temperature needs to be greater than 2369 K for MgO emission to be achieved. Also, UVA emission was shown to be a strong function of stoichiometry. For example, the formulation including Mg/KClO4 produces significant MgO at elevated temperatures to emit well in the UVA. As this mixture becomes increasingly fuel rich, emission intensity is optimized. The additional Mg from the fuel rich mixture combines with oxygen from air to produce greater concentration of MgO that optimize the overall emission intensity. This study provides a foundational understanding on how to use a thermite reaction properties such as adiabatic flame temperature at stoichiometry to engineer a specific response, in this case heightened UVA emission.

LIST OF TABLES

LIST OF FIGURES

CHAPTER I

INTRODUCTION

1.1 Background

Researchers have studied tailored chemistry in pyrotechnic formulations in order to control light emission in discrete wavelength regimes. This is a useful approach for synthesizing a flare, for example, that burns to emit discrete colors that may signify a specific message. In 2015, Sabatini et al. developed a red-light emitting pyrotechnic formulation based solely on the existence of a transient $SrOH_{(g)}$ species. It was achieved by using either 5-amino-1H-tetrazole or hexamine to deoxidize the combustion flame of a $Mg/Sr(NO_3)_2$/Epon-binder composition and reduce the amount of both condensed and gaseous SrO, which emits undesirable orange-red light. The study showed that based only on SrOH, with concomitant SrH emission, both high intensity and highly saturated red flames can be obtained. (Sabatini, Koch and Poret)

In 2011, a green-light-emitting pyrotechnic formulation was developed by Sabatini et al. The formulation was a mixture of potassium nitrate, boron carbide, and an epoxy binder. Green-light-emission occurred owing to the formation and emission of metastable boron dioxide (BO_2). (Sabatini, Poret and Broad, Boron Carbide as a Barium-Free Green Light Emitter and Burn-Rate Modifier in Pyrotechnics) In 2014, improved green-light-emitting pyrotechnic formulations were developed to ameliorate the relatively low spectral purity of the aforementioned formulation. Tris(2,2,2-trinitroethyl)-borate (TNEB) was determined to be a suitable oxidizing material with an oxygen balance of +13.1. By means of replacing potassium nitrate with TNEB in the presence of boron carbide, magnesium, and paraffin wax, a green-light-emitting pyrotechnic formulation with high performance and spectral purity was obtained. (Klapötke, Krumm and Rusan)

Blue-light emission in pyrotechnics is very challenging and requires the exact tuning of different parameters such as the specific ratio of the ingredients, reactivity, and combustion temperature. In 2014, another suitable blue-light emission was

synthesized through the generation of molecular emitting copper(I) iodide to substitute for copper(I) chloride (CuCl). Replacing the chloride containing reactant was desirable because CuCl is especially unstable. However, CuI is known to emit in the blue region at 460 nm spectroscopically. The $Cu(IO_3)_2$ was determined to serve as a suitable oxidizer for achieving the generation of blue flame based on molecular copper(I) iodide, as it can also form this light emitter during the combustion process. The best blue-light-emitting pyrotechnic formulation is a mixture of copper iodate/magnesium/guanidine nitrate, with urea or copper serving as an additional fuel source. (Klapötke, Rusan and Sabatini, Chlorine-Free Pyrotechnics: Copper(I) Iodide as a "Green" Blue-Light Emitter)

1.2 Objective

All of these studies demonstrate that pyrotechnic formulations that emit well for specific colors in the visible region can be achieved by selecting specific species that are known to emit well in the wavelength of interest. The art to tailoring the formulation is recognizing how to best create the emitting species *in-situ* reaction. The current work is an extension of previous studies with the goal to formulate a pyrotechnic mixture that emits strongly in the ultraviolet (UV) specifically, the UVA spectrum (i.e., 315-400 nm). Towards this end, many formulations were examined experimentally and all were based on either aluminum fuel or magnesium fuel based mixtures. Several solid oxidizers were studied in combination with the fuel powder. Small quantities of pyrotechnic mixtures were prepared and ignited using a hot wire. The emission spectra of each reaction was recorded using a UV-VIS spectrometer. Further analysis of reaction temperatures helped elucidate possible mechanisms for strong emission in specific formulations. These results provide a distinct recipe for creating a strongly emitting UVA pyrotechnic.

CHAPTER II

EXPERIMENTAL

2.1 Materials

Two fuel powders were examined separately in this study: aluminum (Al) and magnesium (Mg). The Al powder was supplied by Novacentrix (Austin, TX), has an average spherical particle diameter of 80 nm, and is encapsulated in a 2-4 nm amorphous Al_2O_3 passivation shell. The micron-size (< 45 μm) Mg powder was supplied by Alfa Aesar, is also spherical and passivated by a 4 nm thick MgO shell. Table 1 summarizes these fuel powders and all oxidizer powders examined including the particle size and supplier. The oxidizers included potassium perchlorate ($KClO_4$), potassium permanganate ($KMnO_4$), diiodine pentoxide (I_2O_5), molybdenum(VI) trioxide (MoO_3), iron(III) oxide (Fe_2O_3), polytetrafluoroethylene (PTFE), copper(II) oxide (CuO), zinc oxide (ZnO), manganese(II) oxide (MnO), and sodium perchlorate ($NaClO_4$). It is noted that the I_2O_5 powder had to be ground using a mortar and pestle to reduce particle size and aid intermixing with the fuel powders.

Seventeen mixtures with Al or Mg as the fuel and $KClO_4$, $KMnO_4$, I_2O_5, MoO_3, Fe_2O_3, PTFE, CuO, ZnO, MnO, and $NaClO_4$ as the oxidizers, respectively, at different equivalence ratios (ϕ) were examined and are summarized in Table 2. The combustion properties reported in Table 2 are calculated from REAL code, a thermal equilibrium software program. These properties are included to provide a general gauge for how each mixture may produce different adiabatic flame temperatures and gas generation. For the specified ϕ, the mixtures were prepared using the requisite amount of powder suspended in hexane that is used as a carrier fluid aiding intermixing of the reactants. The suspension was sonicated using a Misonix Sonicator 3000 sonic wand for a total time of 1 min with a 10 s on/off intervals to avoid heating the solution. The sonication process promotes homogeneous mixing of the powders. The suspension was transferred into a Pyrex dish in a vacuum oven to evaporate the hexane. Once evaporated, the dried powders were reclaimed for further experimentation.

Table 1. Material details including supplier and average particle size

Material	Average particle size	Supplier
Aluminum (Al)	80 nm	Novacentrix
Magnesium (Mg)	< 45 μm	Alfa Aesar
Potassium perchlorate ($KClO_4$)	150 μm	Sigma-Aldrich
Potassium permanganate ($KMnO_4$)	≤ 150 μm	Sigma-Aldrich
Diiodine pentoxide (I_2O_5)	150 μm	Sigma-Aldrich
Molybdenum(VI) trioxide (MoO_3)	> 1 μm	Alfa Aesar
Iron(III) oxide (Fe_2O_3)	< 50 nm	Sigma-Aldrich
Polytetrafluoroethylene (PTFE MP1400)	10 μm	DuPont
Copper(II) oxide (CuO)	< 50 nm	Sigma-Aldrich
Zinc oxide (ZnO)	< 50 nm	Sigma-Aldrich
Manganese(II) oxide (MnO)	≥ 74 μm	Alfa Aesar
Sodium perchlorate ($NaClO_4$)	150 μm	Sigma-Aldrich

Table 2. Equivalence ratio and flame temperature for the specified formulation examined. Combustion properties evaluated using thermal equilibrium software, REAL

Reaction	Equivalence ratio (ϕ)	Adiabatic flame temperature (K)
Al/I_2O_5	1	3876
$Al/KClO_4$	1	3849
Al/MoO_3	1	3847
$Al/NaClO_4$	1	3833
Al/PTFE	1	3422
$Al/KMnO_4$	1	3184
Al/Fe_2O_3	1	3133
Al/CuO	1	2839
Al/MnO	1	2062
Al/ZnO	1	1485

Reaction	Equivalence ratio (ϕ)	Adiabatic flame temperature (K)
$Mg/KClO_4$	1.2	3296
$Mg/KClO_4$	1	3294
$Mg/KClO_4$	1.4	3280
$Mg/KClO_4$	0.8	3267
$Mg/KClO_4$	1.6	3247
$Mg/KClO_4$	0.6	3196
Mg/MnO	1	2369

2.2 Spectrometer Experiments

Figure 1 shows the setup for the ultraviolet emission experiments using a STS-UV Ocean Optics 2000 (Dunedin, FL) emission and absorption spectrometer with range from 190 to 650 nm wavelength. Each 50 mg sample was placed in the shallow depression on the acrylic plate in the combustion chamber. A Nichrome wire was connected to the powder and power supply to provide resistive heating and ignition of the sample. The voltage was maintained at 15 V for each test. Figure 1 also shows a cosine corrector and fiber optic cable (Ocean Optics) used to collect signal from a 180° field of view. The fiber optic cable was mounted on the acrylic plate along the centerline, aligned with the center of the sample and covered with a sapphire lens for protection (sapphire is highly transparent to UV wavelengths). The distance between the lens and sample was constant at 10.4 cm. On ignition, the wavelength specific intensity of UV light emitted by the reaction was recorded by the spectrometer and data acquisition system. Three tests were conducted for each mixture in order to monitor repeatability. During experimentation, care was taken to reduce light emission and reflection from all the surfaces of the apparatus. The walls of the combustion chamber were painted black such that inside the chamber was fully dark. The experimental setup was purposefully isolated from sources of stray light that can decrease the signal-to-noise ratio.

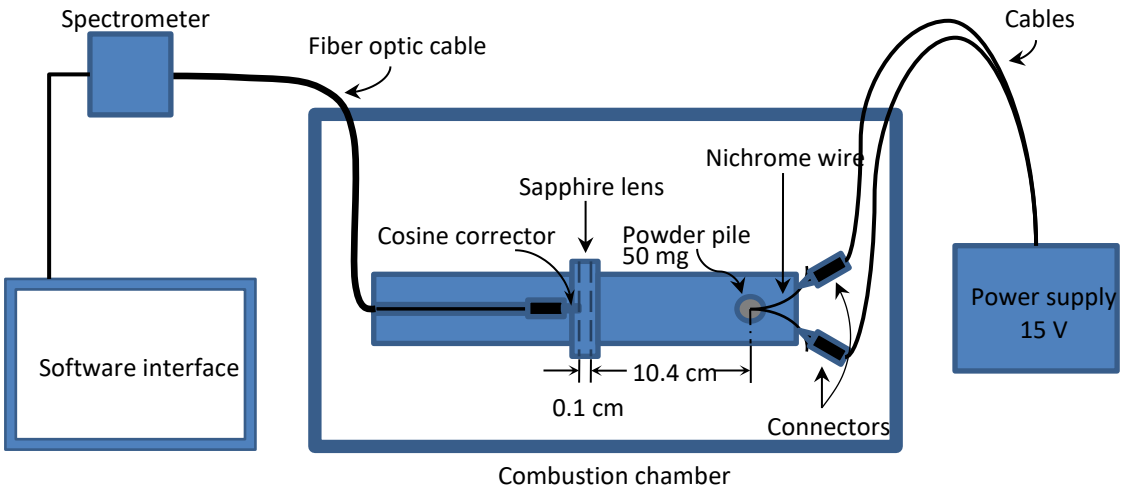

Figure 1. Schematic diagram of the ultraviolet emission experimental setup.

CHAPTER III

RESULTS & DISCUSSION

Figure 2 shows the emission intensity as a function of wavelength for all the mixtures. Of the 17 different mixtures examined, there is a distinct separation between the mixtures containing Al compared Mg. Specifically, Figure 3 shows the spectra associated with Al fuel while Figure 4 shows the spectra associated with Mg fuel. In both Figure 3 and 4, many discrete species emissions are identified but the distinction can be seen in Figure 4 starting at about 360 nm and ending at about 400 nm. All Mg containing formulations that also include potassium produce a pronounced broad emission peak indicative of greater emission intensity in this UVA region.

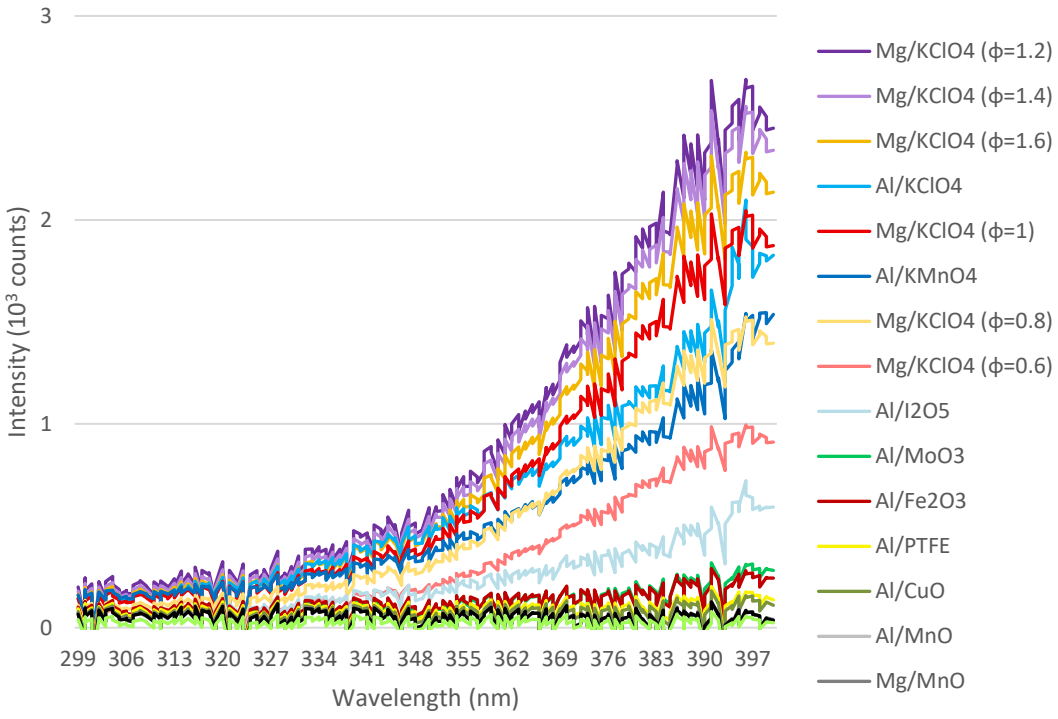

Figure 2. Emission spectrum intensity as a function of wavelength for all mixtures identified in graph. The legend is in order of intensity at 395 nm wavelength. $\phi = 1.0$ if not labeled.

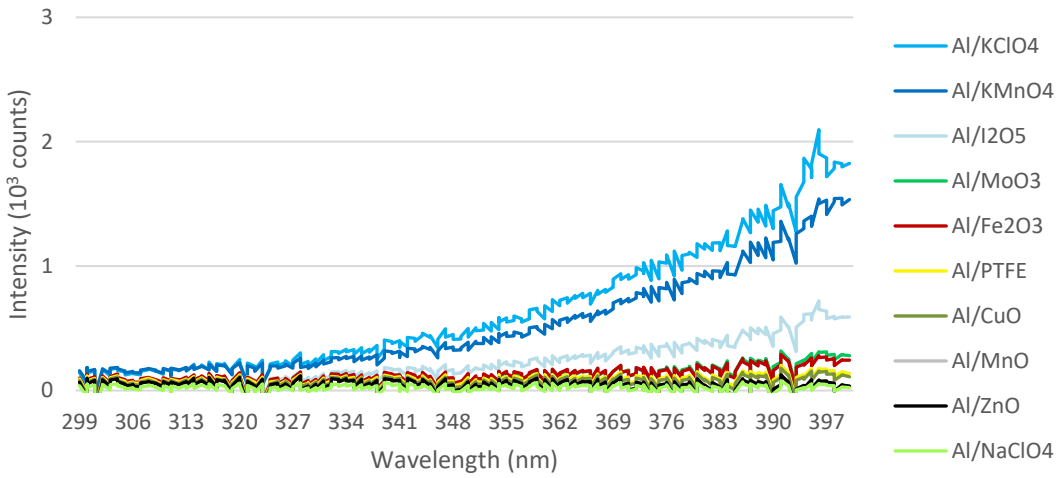

Figure 3. Emission spectrum intensity as a function of wavelength for mixtures whose fuel is aluminum (Al) in the UVA. $\phi = 1.0$ if not labeled.

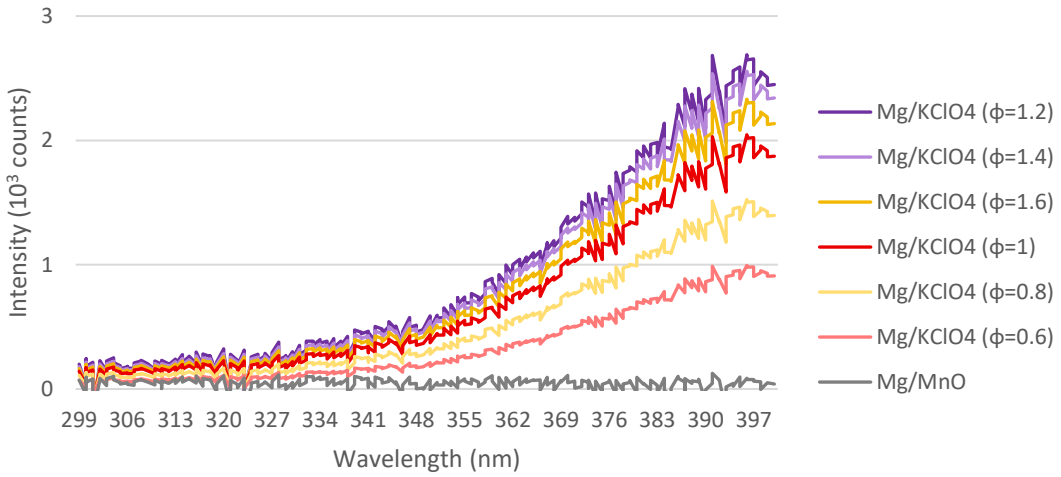

Figure 4. Emission spectrum intensity as a function of wavelength for mixtures whose fuel is magnesium (Mg) in the UVA.

Figure 5 shows the gradient of intensity for the wavelength range of 350-390 nm. The intensity was compared among all mixtures based on the gradients in Figure 2-4. The mixtures having the four steepest gradients were all $Mg/KClO_4$ consistent with the observation of higher emission intensity in the UVA for this formulation.

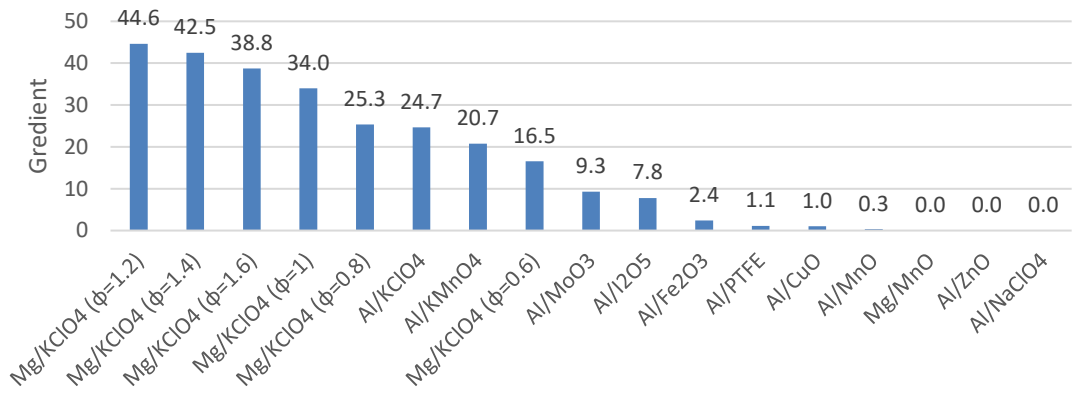

Figure 5. Gradient of intensity over the wavelength range of 350-390 nm for all mixtures.

Thermal equilibrium code analysis on Al/$KClO_4$ ($\phi = 1$), Mg/MnO ($\phi = 1$), and Mg/$KClO_4$ reactions for $\phi = 0.6, 0.8, 1.0, 1.2, 1.4, 1.6$ are shown in Figure 6. This analysis of Figure 6 indicates commonalities among product species that correlate with high UVA emission. For example, the concentration of MgO for every ratio of Mg/$KClO_4$ is high but the potassium (K) and/or chlorine (Cl) containing species for both mixtures are relatively similar. Therefore, the K and Cl containing species are likely not responsible for the prominent peak in the UVA otherwise Al/$KClO_4$ ($\phi = 1$) would also demonstrate this peak. Figure 6 suggests that the prominent emission in the UVA may be attributed to Mg containing species, such as MgO in both the gas and condensed phase (Sabatini, Koch and Poret). Figure 6b further elucidates Mg/$KClO_4$ concentration variations as a function of ϕ. There is a significant abundance of MgO in the condensed phase for every ϕ examined, consistent with the emission spectra in the UVA.

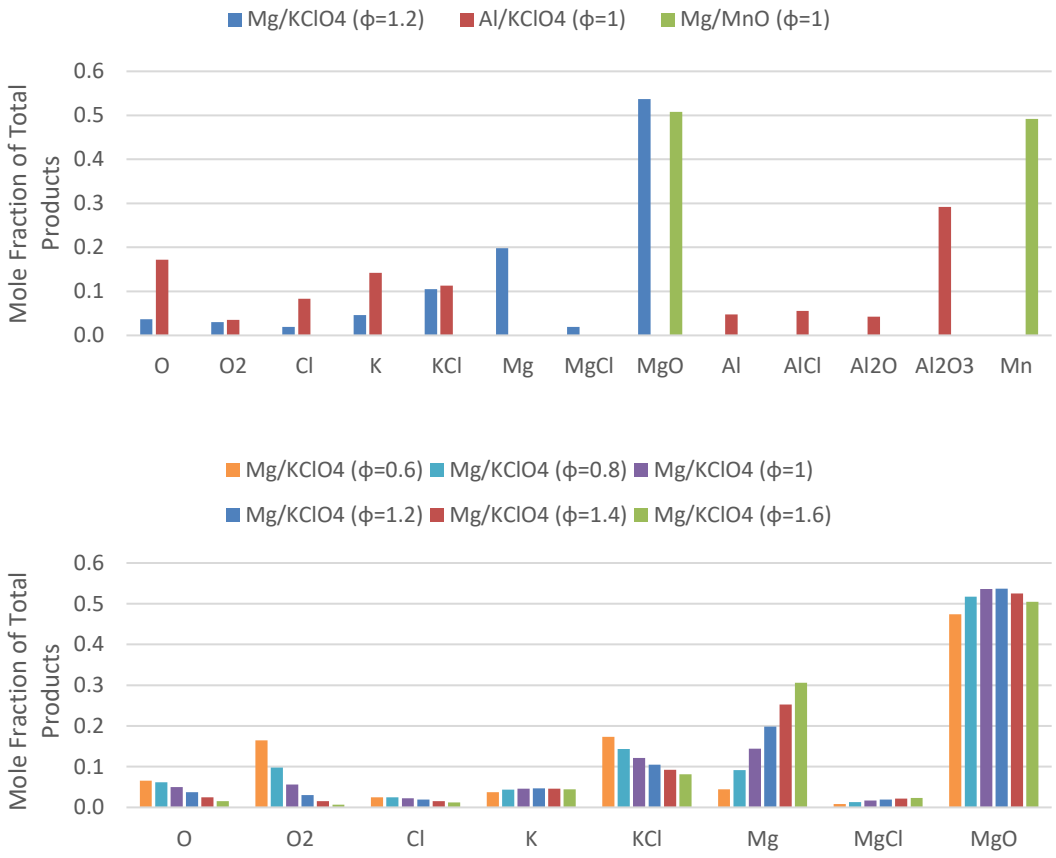

Figure 6. Reaction products for Al/$KClO_4$ of ϕ = 1, Mg/MnO of ϕ = 1, and Mg/$KClO_4$ of ϕ = 0.6, 0.8, 1.0, 1.2, 1.4, 1.6.

Figure 7 shows the flame temperature and emission intensity at 395 nm for Mg/$KClO_4$ as a function of ϕ. Both the optimized values of flame temperature (3296 K) and emission intensity for Mg/$KClO_4$ are at ϕ = 1.2. Coincidently ϕ = 1.2 also corresponds with the highest concentration of $MgO_{(g)}$ in the products. This elevated temperature would naturally promote more MgO vaporization in the products and this could contribute to heightened emission intensity in the UVA (as shown in Figure 7). This argument is consistent with the comparison between temperature, emission intensity and $MgO_{(g)}$ concentration for ϕ = 1.4; but not in the case of ϕ = 1.0. At stoichiometry the interesting observation from Figure 6b is that there is a significant

decrease in Mg product species. This implies that Mg may also contribute to higher levels of emission intensity in the UVA.

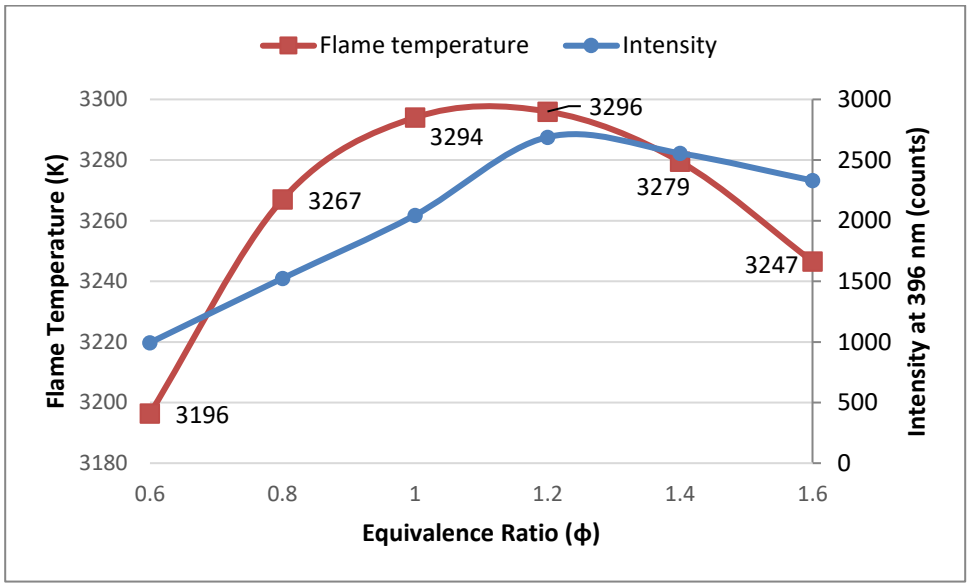

Figure 7. Adiabatic flame temperature and emission intensity at 395 nm of Mg/$KClO_4$ versus ϕ.

Magnesium emits radiation as a triplet at 383-384 nm. (Koch) Magnesium burning in air generates a high concentration of MgO that emits ultraviolet radiation at 360-400 nm. (Barrow and Crawford) . In Figure 7, the fuel rich samples emission intensity increases significantly compared with the stoichiometric and fuel lean samples. The significant increase in emission intensity may be a result of additional reactions between Mg and oxygen from the environment to produce MgO. Thermal equilibrium code analysis was further pursued to estimate the increase in MgO concentration as a function of additional Mg in a fuel rich mixture (i.e., e = 1.2) reacting with oxygen from the environment. The analysis of Figure 8 shows a significant increase in MgO concentration that the analysis in Figure 7 did not include for the fuel rich samples. Therefore, fuel rich samples exhibit higher emission intensity in the UVA that can be attributed to the combustion synthesis of greater

concentrations of MgO at elevated temperatures (i.e., > 3196 K). The elevated temperature is an important criterion for UVA emission of MgO; otherwise the Mg/MnO reaction would exhibit high UVA emission and it does not. Figure 4 shows that the Mg/MnO reaction does not emit well in the UVA though this reaction also produces MgO (Figure 6a). Overall, for the purpose of optimizing UVA emission, magnesium is a better fuel than aluminum. For comparison, Al and Mg melt at similar temperatures (660 °C (Hasan) compared with 650 °C (Schaum and Burnett), respectively), but Mg boils at a lower temperature (2467 °C (Hasan) for Al compared with 1110 °C (Schaum and Burnett) for Mg). The thermodynamics associated with phase change enables Mg to oxidize more readily in the vapor phase therefore produce more MgO in the condensed and vapor phase. Similarly, $KClO_4$ melts at a lower temperature than MnO (525 °C (Lide) for $KClO_4$ compared with 1842 °C (Lide) for MnO). MnO will not exist in liquid or gas phase until the temperature reaches higher values. The reaction of Mg/MnO does not start until the temperature reaches 2115 K (1842 °C) which is just below 2396 K, the flame temperature of Mg/MnO reaction, while the reaction of Mg/$KClO_4$ starts earlier since both melting points of Mg and $KClO_4$ are relatively low. Therefore, $KClO_4$ is a better oxidizer for both Al and Mg than MnO.

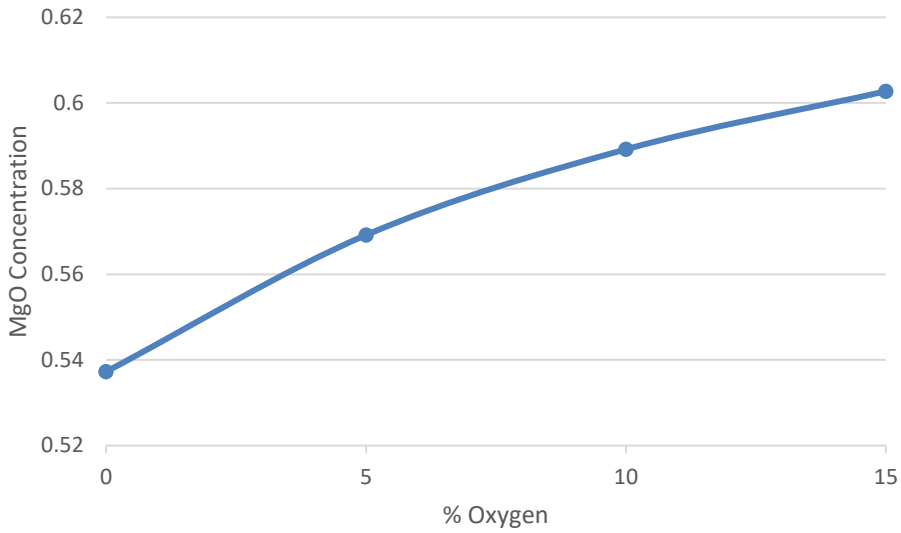

Figure 8. Thermal equilibrium REAL code analysis of $\phi = 1.2$ Mg/$KClO_4$ product species MgO with various concentrations of added oxygen representing environmental oxygen contributions to the reaction. Note the increase in MgO concentration with oxygen from environment participates in the reaction.

The MgO in condensed phase is white cubic crystalline, and it is rock-salt structure. (Langjahr, Wagner and Lange) The surface oxygen ions at edges and corners have reduced coordination compared with bulk (shown in Figure 9). (Di Cosimo, Díez and Ferretti) Therefore, it creates reduction in the energy gap between the highest occupied molecular orbital (HOMO) and the lowest unoccupied molecular orbital (LUMO) states. Because the combustion process is so quick and the integration time is so short for each spectrometer test that the product MgO crystallites are in nano size, the surface-to-volume ratio is large. Therefore, a few more states are created within the energy band gap. (Wu, Truong and Goodman; Trevisanutto, Sushko and Shluger) The HOMO state is basically localized to the surface oxygen anions, and the LUMO state is delocalized and extends to the adjacent magnesium cations. When the excitation process occurs, the electron jumps from surface oxygen to adjacent magnesium. Once the electron goes back to oxygen, emission occurs. The emission bands from 2.7-3.2 eV is attributed to 3-coordinated sites, and the emission bands from 3.2-3.7 eV is attributed to 4-coordinated sites. (Coluccia, Tench and Segall;

Bailly, Costentin and Lauron-Pernot) Therefore, the optical properties of MgO have been explained on the charge transfer occurring at low coordination sites. (Selvamani, Sinhamahapatra and Bhattacharjya; Kumar, SubhashThota and ShikhaVarma; Sterrer, Berger and Diwald; Kumar, Kumar and Priya, Defect and Adsorbate Induced Ferromagnetic Spin-order in Magnesium Oxide Nanocrystallites; Zhang and Zhang)

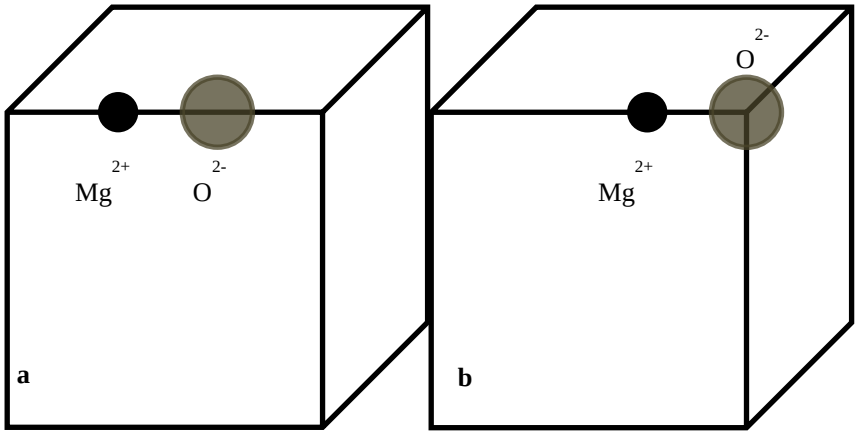

Figure 9. Schematic of differently coordinated surface oxygen anions on MgO particles: (a) 4-coordinated oxygen anions in edge and (b) 3-coordinated oxygen anions in corner.

CHAPTER IV

CONCLUSIONS

All the best formulations among 17 mixtures contain Mg. The mixture emitting best in the UVA among all tested mixtures is $Mg/KClO_4$ at $\phi = 1.2$. Magnesium burning in air generates a lot amount of both gaseous and condensed phase of MgO which has a complex series of bands in at 360-400 nm the UVA. The charge transfer occurring at low coordinate sites on the MgO surface contributes to emission at 335-400 nm in the UVA. Magnesium is better as a fuel than aluminum for emission in the UVA. The adiabatic flame temperature is also an important factor influence the value of emission intensity.

BIBLIOGRAPHY

Bailly, Marie-Laurence, et al. "Physicochemical and in Situ Photoluminescence Study of the Reversible Transformation of Oxide Ions of Low Coordination into Hydroxyl Groups upon Interaction of Water and Methanol with MgO." *J. Phys. Chem. B* 109.6 (2005): 2404-2413.

Barrow, R. F. and D. V. Crawford. "A Note On the Spectrum of MgO." *Proceedings of the Physical Society* 57.1 (1945): 12-15.

Coluccia, Salvatore, Anthony J. Tench and obert L. Segall. "Surface Structure and Surface States in Magnesium Oxide Powders." *J. Chem. Soc., Faraday Trans. 1* 75 (1979): 1769-1779.

Di Cosimo, J. I., et al. "Basic Catalysis on MgO: Generation, Characterization and Catalytic Properties of Active Sites." *Catalysis* 26 (2014): 1-28.

Hasan, Heather. *Aluminum (Understanding the Elements of the Periodic Table)*. New York: The Rosen Publishing Group, 2007.

Klapötke, Thomas M., et al. "Boron Carbide as a Barium-Free Green Light Emitter and Burn-Rate Modifier in Pyrotechnics." *Chemical Communications* 50.67 (2014): 9581-9583.

Klapötke, Thomas M., Magdalena Rusan and Jesse J. Sabatini. "Chlorine-Free Pyrotechnics: Copper(I) Iodide as a “Green” Blue-Light Emitter." *Angewandte Chemie International Edition* 53.36 (2014): 9665-9668.

Koch, Ernst-Christian. *Metal-fluorocarbon Based Energetic Materials*. Weinheim: Weinheim Germany : Wiley-VCH, 2012.

Kumar, Ashok, et al. "Sol–gel Synthesis of Highly Luminescent Magnesium Oxide Nanocrystallites." *Journal ofLuminescence* 131.4 (2011): 640-648.

Kumar, Ashok, Jitendra Kumar and Shashank Priya. "Defect and Adsorbate Induced Ferromagnetic Spin-order in Magnesium Oxide Nanocrystallites." *Applied Physics Letters* 100.19 (2012): 192404.

Langjahr, Petra A., et al. "Epitaxial Growth and Structure of Highly Mismatched Oxides With Rock-salt Structure on MgO." *Journal of Crystal Growth* 256.1-2 (2003): 162-173.

Lide, David R. *CRC Handbook of Chemistry and Physics*. Boca Raton: CRC Press/Taylor & Francis Group, 2007.

Sabatini, Jesse J., et al. "Chlorine-Free Red-Burning Pyrotechnics." *Angewandte Chemie International Edition* 54.37 (2015): 10968-10970.

Sabatini, Jesse J., Jay C. Poret and Russell N. Broad. "Boron Carbide as a Barium-Free Green Light Emitter and Burn-Rate Modifier in Pyrotechnics." *Angewandte Chemie (International ed. in English)* 50.20 (2011): 4624–4626.

Schaum, J.H. and H. C. Burnett. "Magnesium-Rich Side of the Magnesium-Zirconium Constitution Diagram." *Research of the National Bureau of Standards* 49.3 (1952): 155-162.

Selvamani, T., et al. "Rectangular MgO Microsheets with Strong Catalytic Activity." *Materials Chemistry and Physics* 129.3 (2011): 853-861.

Sterrer, Martin, et al. "Energy Transfer on the MgO Surface, Monitored by UV-induced H2 Chemisorption." *Journal of the American Chemical Society* 125.1 (2002): 195-199.

Trevisanutto, P. E., et al. "A Mechanism of Photo-induced Desorption of Oxygen Atoms from MgO Nano-crystals." *Surface Science* 593.1-3 (2005): 210-220.

Wu, Ming-Cheng, Charles M. Truong and D. Wayne Goodman. "Electron-energy-loss-spectroscopy Studies of Thermally Generated Defects in Pure and Lithium-doped MgO(100) Films on Mo(100)." *Physical Review B* 46.19 (1992): 12688-12694.

Zhang, Jun and Lide Zhang. "Intensive Green Light Emission from MgO Nanobelts." *Chemical Physics Letters* 363.3 (2002): 293-297.